iScience

CellPress
OPEN ACCESS

Article

Nuclear translocation of cleaved PCDH9 impairs gastric cancer metastasis by downregulating CDH2 expression

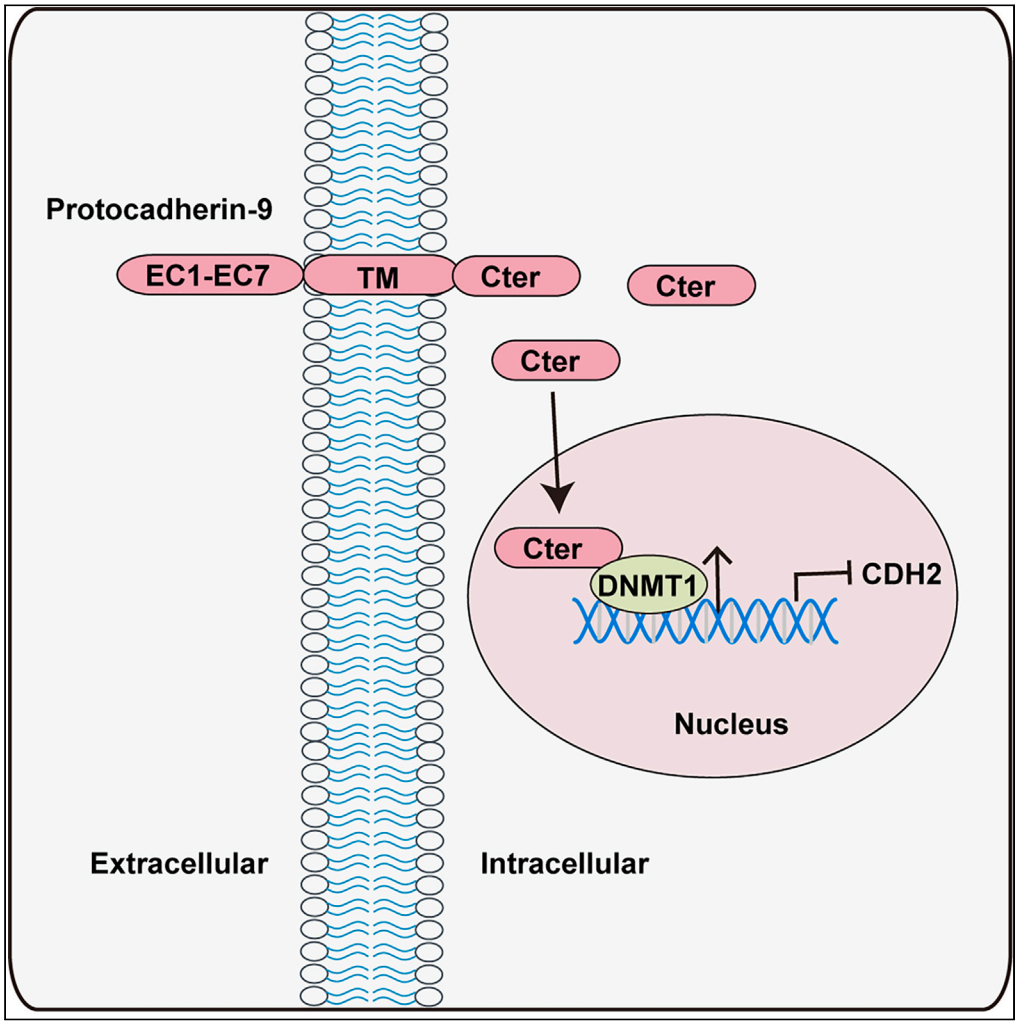

Yajuan Zhang, Yingwei Zhu, Ying Chen, ..., Hong Gao, Weiwei Yang, Guanzhen Yu

zhangyajuan2013@sibcb.ac.cn (Y.Z.)
wyang@sibcb.ac.cn (W.Y.)
qiaoshanqian@aliyun.com (G.Y.)

Highlights

PCDH9 is cleaved and translocates into nucleus to inhibit gastric cancer metastasis

Nuclear PCDH9 activates DNMT1 to repress *CDH2* expression

Nuclear PCDH9 levels correlate with the prognosis of gastric cancer patients

Zhang et al., iScience *27*, 109011
February 16, 2024
https://doi.org/10.1016/j.isci.2024.109011

iScience

CellPress
OPEN ACCESS

Article

Nuclear translocation of cleaved PCDH9 impairs gastric cancer metastasis by downregulating CDH2 expression

Yajuan Zhang,[1,2,10,*] Yingwei Zhu,[3,10] Ying Chen,[4,10] Yanli Wang,[5,10] Bing Liu,[2] Yating Pan,[6] Xinyi Liao,[6] Jun Pan,[7] Hong Gao,[2] Weiwei Yang,[2,8,*] and Guanzhen Yu[6,9,11,*]

SUMMARY

Loss of Protocadherin 9 (PCDH9) is associated with the metastasis and the prognosis of gastric cancer patients, while the molecular mechanism of PCDH9-impaired gastric cancer metastasis remains unclear. Here we show that PCDH9 is cleaved in gastric cancer cells. Intracellular domain of PCDH9 translocates into nucleus, where it interacts with DNA methyltransferase 1 (DNMT1) and increases DNMT1 activity. Activated DNMT1 downregulates cadherin 2 (*CDH2*) expression by increasing DNA methylation at its promoter, thereby dampening the migration and *in vivo* metastasis of gastric cancer cells. In addition, the levels of nuclear PCDH9 correlate with CDH2 expression, lymph node metastasis, and the prognosis of gastric cancer patients. Our finding demonstrates a unique mechanism of nuclear PCDH9-impaired gastric cancer metastasis by promoting DNA methylation of *CDH2* promoter.

INTRODUCTION

Gastric cancer is a highly prevalent cancer and the third leading cause of cancer-associated death worldwide.[1,2] Although they differ in etiology and the management approaches between the East and the West,[3] the prognostic outcome for gastric cancer patients remains poor, especially in advanced stages.[4,5] The main reason lies in the high rate of locoregional and distant recurrence due to the high ability of invasion and metastasis of gastric cancer cells. Even after radical resection of gastric cancer, the locoregional and distant recurrences are common, being detected in approximately 50% of patients. Systemic chemotherapy did not impose any impact on either locoregional or distant recurrence.[5,6] The status of gastric wall erosion and lymph node metastasis at diagnosis contributes to recurrence after radical resection of gastric cancer. Therefore, understanding the many biological markers in differential signaling pathways and processes involved in metastasis will highlight effective and targeted therapeutic strategies to prevent and treat gastric cancer metastasis.

Metastasis is a dynamic succession of events involving the escape of cancer cells from the primary tumor, followed by circulation in the blood or lymph system, and ultimately colonizing in distant organs.[7,8] Metastatic process of tumors required a number of random genetic and epigenetic alterations in cancer cells combined with diverse interactions between cancer cells and their microenvironment.[9] Genes responsible for each individual step along the metastatic process have been extensively studied and are partially identified, aiding in the development of rational antimetastatic strategies.[10,11] Targeting metastasis-specific genes has already been adopted as a treatment for solid tumors. Vascular endothelial growth factor (VEGF) signaling plays a significant role in metastasis initiation. Bevacizumab, targeting VEGF, has been widely used clinically for patients with advanced colorectal, breast, ovarian, renal, non-small cell lung cancer, and glioblastoma.[12] Denosumab, a humanized monoclonal antibody targeting receptor activator of NF-κB ligand (RANKL), is another promising potential antimetastatic drug.[13] Although multiple agents have been demonstrated to prevent or shrink metastases, the preclinical and clinical results are not always optimistic. In-depth understanding of metastasis pathways will hold promise for identifying druggable pathways and then enhance the efficacy of current treatments.[13]

Protocadherin 9 (PCDH9) is a member of non-clustered protocadherins (PCDHs) and belongs to the cadherin family. The non-clustered PCDHs appear to have homophilic/heterophilic cell-cell adhesion properties, and some have been suggested as candidate tumor suppressor

[1]Shanghai Institute of Thoracic Oncology, Shanghai Chest Hospital, Shanghai Jiao Tong University School of Medicine, Shanghai 200030, China
[2]State Key Laboratory of Cell Biology, Shanghai Institute of Biochemistry and Cell Biology, Center for Excellence in Molecular Cell Science, Chinese Academy of Sciences, University of Chinese Academy of Sciences, Shanghai 200031, China
[3]Department of Gastroentrology, Jiangnan University Medical Center, Wuxi 214000, China
[4]Department of Gastroenterology, Changhai Hospital, Naval Medical University, Shanghai 200003, China
[5]Department of Pathology, Fudan University Shanghai Cancer Center, Shanghai 200032, China
[6]Department of Oncology, Longhua Hospital Affiliated to Shanghai University of Traditional Chinese Medicine, Shanghai 200032, China
[7]Department of Medical Oncology, Cancer Center of Jinling Hospital, Nanjing 210002, China
[8]Key Laboratory of Systems Health Science of Zhejiang Province, School of Life Science, Hangzhou Institute for Advanced Study, University of Chinese Academy of Sciences, Hangzhou 310024, China
[9]Medical Artificial Intelligence Laboratory, Zhejiang Institute of Digital Media, Chinese Academy of Science, Shaoxing 312366, China
[10]These authors contributed equally
[11]Lead contact
*Correspondence: zhangyajuan2013@sibcb.ac.cn (Y.Z.), wyang@sibcb.ac.cn (W.Y.), qiaoshanqian@aliyun.com (G.Y.)
https://doi.org/10.1016/j.isci.2024.109011

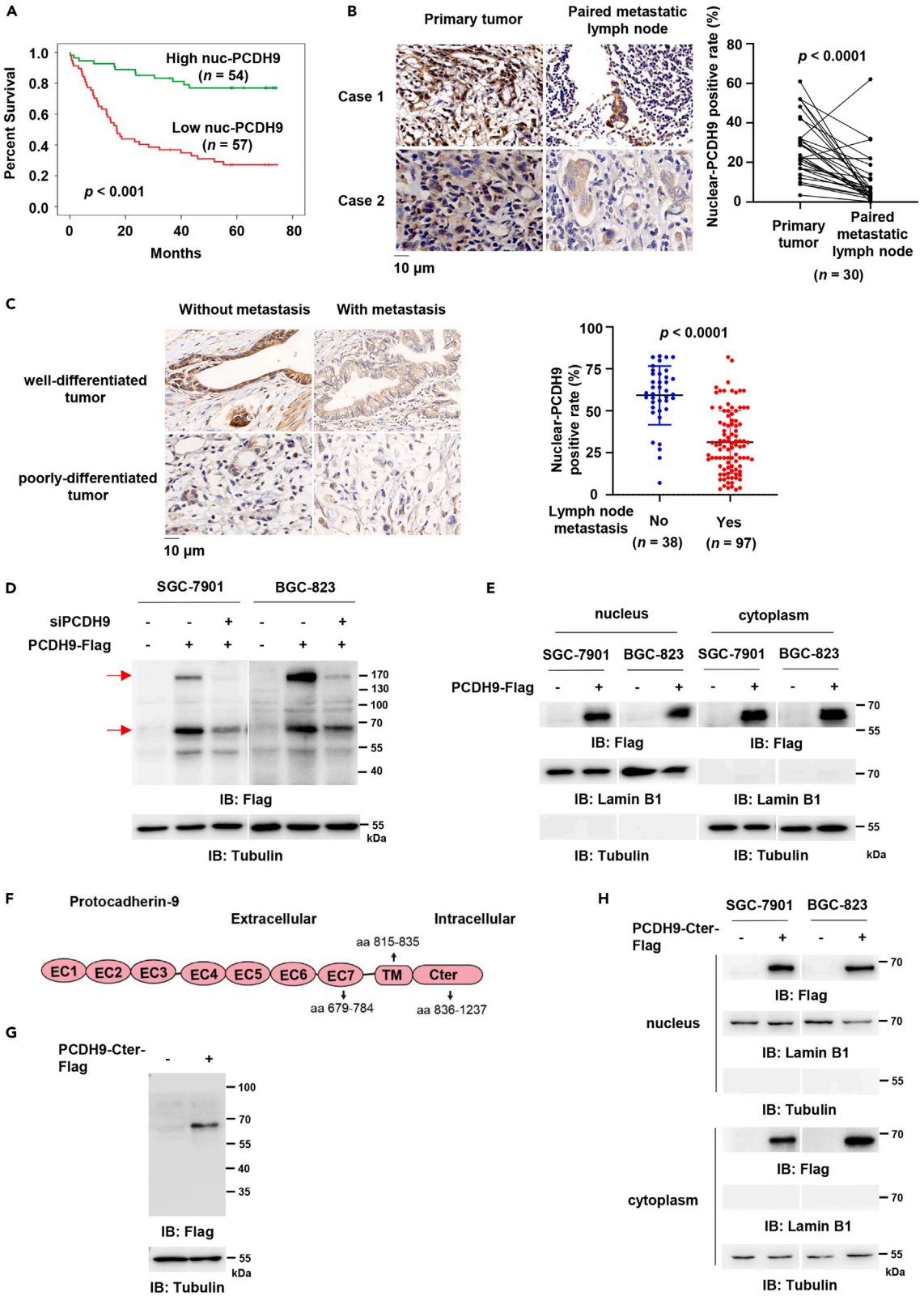
A
Percent Survival
1.0
0.8
0.6
0.4
0.2
0.0
High nuc-PCDH9
(n = 54)
Low nuc-PCDH9
(n = 57)
p < 0.001
0
20
40
60
80
Months
B
Primary tumor
Paired metastatic lymph node
Case 1
Case 2
10 μm
Nuclear-PCDH9 positive rate (%)
80
60
40
20
0
p < 0.0001
Primary tumor
Paired metastatic lymph node
(n = 30)
C
Without metastasis
With metastasis
well-differentiated tumor
poorly-differentiated tumor
10 μm
Nuclear-PCDH9 positive rate (%)
100
75
50
25
0
p < 0.0001
Lymph node metastasis
No
(n = 38)
Yes
(n = 97)
D
SGC-7901
BGC-823
siPCDH9
PCDH9-Flag
170
130
100
70
55
40
IB: Flag
55
kDa
IB: Tubulin
E
nucleus
cytoplasm
SGC-7901
BGC-823
SGC-7901
BGC-823
PCDH9-Flag
70
55
IB: Flag
IB: Flag
70
IB: Lamin B1
IB: Lamin B1
55
IB: Tubulin
IB: Tubulin
kDa
F
Protocadherin-9
Extracellular
Intracellular
aa 815-835
EC1
EC2
EC3
EC4
EC5
EC6
EC7
TM
Cter
aa 679-784
aa 836-1237
G
PCDH9-Cter-Flag
100
70
55
40
35
IB: Flag
55
kDa
IB: Tubulin
H
SGC-7901
BGC-823
PCDH9-Cter-Flag
70
IB: Flag
nucleus
70
IB: Lamin B1
55
IB: Tubulin
70
IB: Flag
cytoplasm
70
IB: Lamin B1
55
kDa
IB: Tubulin

Figure 1. Nuclear PCDH9 levels correlate with metastasis of gastric cancer

(A) IHC staining using anti-PCDH9 C-terminal antibody was performed in tumor tissues of gastric cancer patients. Survival duration of patients with gastric cancer with high (n = 54, green curve) or low (n = 57, red curve) nuclear PCDH9 positive rate were compared (two-tailed log rank test).

(B) IHC staining using anti-PCDH9 C-terminal antibody was performed in primary tumors and paired metastatic lymph node tumors from 30 gastric cancer patients. Nuclear positive rates of PCDH9 were compared between primary tumors and paired metastatic tumors. Left, representative images of IHC staining were shown. Right, quantitative scoring was carried out. Data represents the mean ± SD of the two groups (paired, two-tailed Student's *t* test). The scale bar represents 10 μm.

(C) IHC analyses were performed in primary tumors from gastric cancer patients with or without lymph node metastasis using anti-PCDH9 C-terminal antibody. Nuclear positive rates of PCDH9 were compared between the patients with lymph node metastasis (n = 97) and those without lymph node metastasis (n = 38). Left, representative images of IHC staining were shown. Right, quantitative scoring was carried out. Data represents the mean ± SD of the two groups (two-tailed Student's *t* test). The scale bar represents 10 μm.

(D) SGC-7901 or BGC-823 cells stably expressing EV or PCDH9-Flag were transfected with siRNAs targeting non-target (NT) or PCDH9. Immunoblotting analyses were performed.

(E) SGC-7901 or BGC-823 cells stably expressing EV or PCDH9-Flag were harvested and subjected to subcellular fractionation assay. Immunoblotting analysis was performed.

(F) Schematic model of PCDH9.

(G) SGC-7901 cells stably expressing EV or PCDH9-Cter-Flag were harvested and immunoblotting analyses were performed.

(H) SGC-7901 or BGC-823 cells stably expressing EV or PCDH9-Cter-Flag were harvested and subjected to subcellular fractionation assay. See also Figure S1.

genes in several solid tumors.[14] PCDH9 functions as a tumor suppressor in various tumor types, including prostate cancer,[15] gastric cancer,[16] glioma,[17] hepatocellular carcinoma,[18] melanoma,[19] etc. We previously reported that PCDH9 expression was gradually decreased along with tumor cells metastasized and could predict the outcomes of gastric cancer patients.[16] Although the clinical relevance and functions of PCDH9 began to be unveiled, the regulatory properties and molecular mechanism of PCDH9 are still in their infancy and need future study.

In this study, we investigated the role and molecular mechanism of PCDH9 in gastric cancer metastasis and found that PCDH9 was cleaved and translocated into nucleus, where it interacted with and activated DNMT1, thereby downregulating CDH2 expression by increasing DNA methylation and dampening tumor metastasis. These results propose a mechanism of nuclear translocation of PCDH9 associated with cancer biology, particularly invasiveness and metastasis.

RESULTS

The levels of nuclear PCDH9 inversely correlate with the metastasis of gastric cancer patients

PCDH proteins have been frequently shown to be proteolytically cleaved by the γ-secretase complex. This cleavage produces soluble intracellular fragments that have the potential to enter the nucleus and may directly or indirectly influence gene expression.[20–22] To test whether PCDH9 is also cleaved and if so, what is the relationship between the cleaved fragments and the malignancy of human gastric cancer, we performed immunohistochemistry (IHC) analysis of PCDH9 using anti-PCDH9 antibody against N-terminal of PCDH9 (N-terminal) or anti-PCDH9 antibody against C-terminal of PCDH9 (C-terminal) in tumor tissues from gastric cancer patients. We observed that PCDH9 N-terminal was mainly localized in cytoplasm, while PCDH9 C-terminal was localized in both cytoplasm and nucleus (Figures S1A and S1B). Besides, we compared overall survival duration of 111 gastric cancer patients, all of whom received standard radiotherapy and chemotherapy after surgery, with low versus high nuclear positive rates of PCDH9. Patients who had high nuclear positive rates of PCDH9 (54 cases) had a much longer median survival duration than those who had low nuclear positive rates of PCDH9 (57 cases) (Figure 1A). Moreover, nuclear positive rates of PCDH9 were much higher in primary tumor tissues than paired metastasis tissues (Figure 1B). In addition, tumors from patients with lymph node metastasis had much lower nuclear positive rates of PCDH9 than those from patients without lymph node metastasis (Figure 1C). Taken together, these results indicate that PCDH9 is likely cleaved and supports a suppressive role of nuclear PCDH9 in gastric cancer metastasis.

Cleaved PCDH9 is localized in nucleus as well as cytoplasm

To further determine whether PCDH9 was cleaved in gastric cancer cells, we constructed PCDH9-Flag plasmid and stably expressed PCDH9-Flag in SGC-7901 or BGC-823 gastric cancer cells. Then we transfected with small interfering RNA (siRNA) against PCDH9 into these cells. Immunoblotting analysis with anti-Flag antibody showed that PCDH9 was cleaved in gastric cancer cells (Figure 1D). And the main cleaved fragment of PCDH9 (about 70 kDa) was localized in both cytoplasm and nucleus, as indicated in the subcellular fractionation assay (Figure 1E).

We next pinpointed the cleaved fragment of PCDH9. As the molecular weight of the cleaved fragment of PCDH9 was about 70 kDa, we generated three truncated mutants of PCDH9 according to its structural domains, including PCDH9-(EC7-Cter)-Flag, PCDH9-(TM-Cter)-Flag, or PCDH9-Cter-Flag, in which Pro679-Leu1237, Tyr785-Leu1237, or Val836-Leu1237 of PCDH9 was cloned (Figure 1F). We then transfected these plasmids into SGC-7901 cells. Immunoblotting analysis showed that PCDH9-Cter-Flag had similar molecular weight to that of the cleaved PCDH9 (Figures 1G and S1C). Subcellular fraction assay also confirmed that PCDH9-Cter-Flag was localized in both cytoplasm and nucleus (Figure 1H), suggesting that C-terminal was cleaved from PCDH9, some of which was translocated into the nucleus.

Nucleus-translocated cleaved PCDH9 C-terminal inhibits gastric cancer cell migration

To further investigate the role of cleaved PCDH9 in gastric cancer progression, we overexpressed PCDH9-Cter-Flag in SGC-7901 or BGC-823 cells and found that PCDH9-Cter-Flag overexpression did not influence cell proliferation (Figure 2A). In contrast, transwell migration and

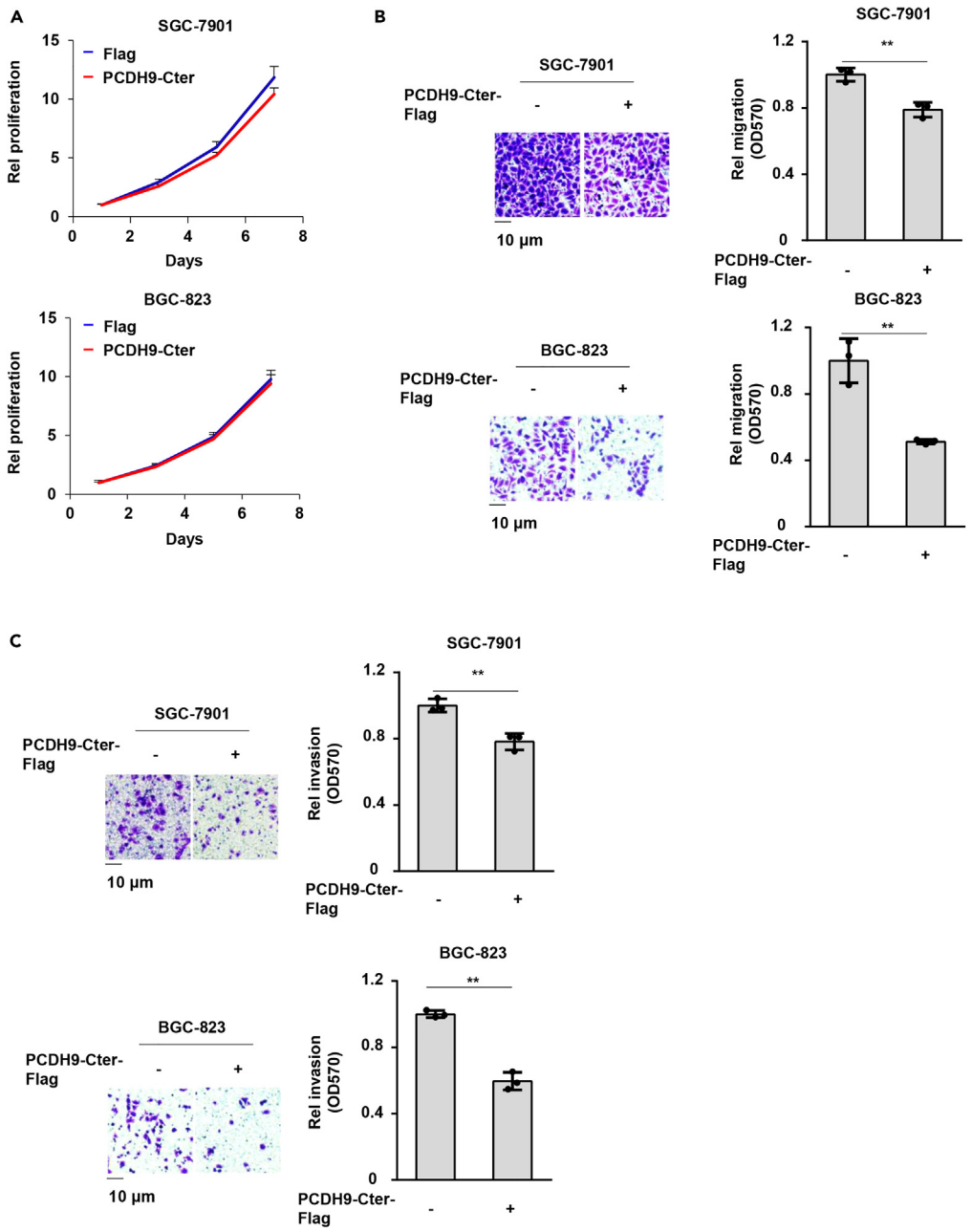

Figure 2. Nucleus-translocated cleaved PCDH9 C-terminal inhibits gastric cancer cell migration

(A) SGC-7901 (top panel) or BGC-823 (bottom panel) cells were infected with the lentivirus expressing EV or PCDH9-Cter-Flag. Cell proliferation assay was performed.

(B) SGC-7901 (top panel) or BGC-823 (bottom panel) cells were infected with the lentivirus expressing EV or PCDH9-Cter-Flag. Transwell migration assays were performed in these cells. Representative images (left) and statistical analyses (right) of the migrated cells were shown.

(C) Transwell invasion assays were performed in these cells in (B). Representative images (left) and statistical analyses (right) of the invaded cells were shown. (A–C) Data represents the mean ± SD of three biologically independent experiments (two-tailed Student's *t* test). *$p < 0.05$, **$p < 0.01$. The scale bar represents 10 μm. See also Figure S2.

invasion assay showed that PCDH9-Cter-Flag overexpression inhibited migration and invasion of SGC-7901 or BGC-823 cells (Figures 2B and 2C).

To test whether nuclear translocation of cleaved PCDH9 was required for its inhibiting cell migration and invasion, we analyzed amino sequence of the PCDH9-Cter with NLStradamus (http://www.moseslab.csb.utoronto.ca/NLStradamus/)[23] and identified a conserved nuclear

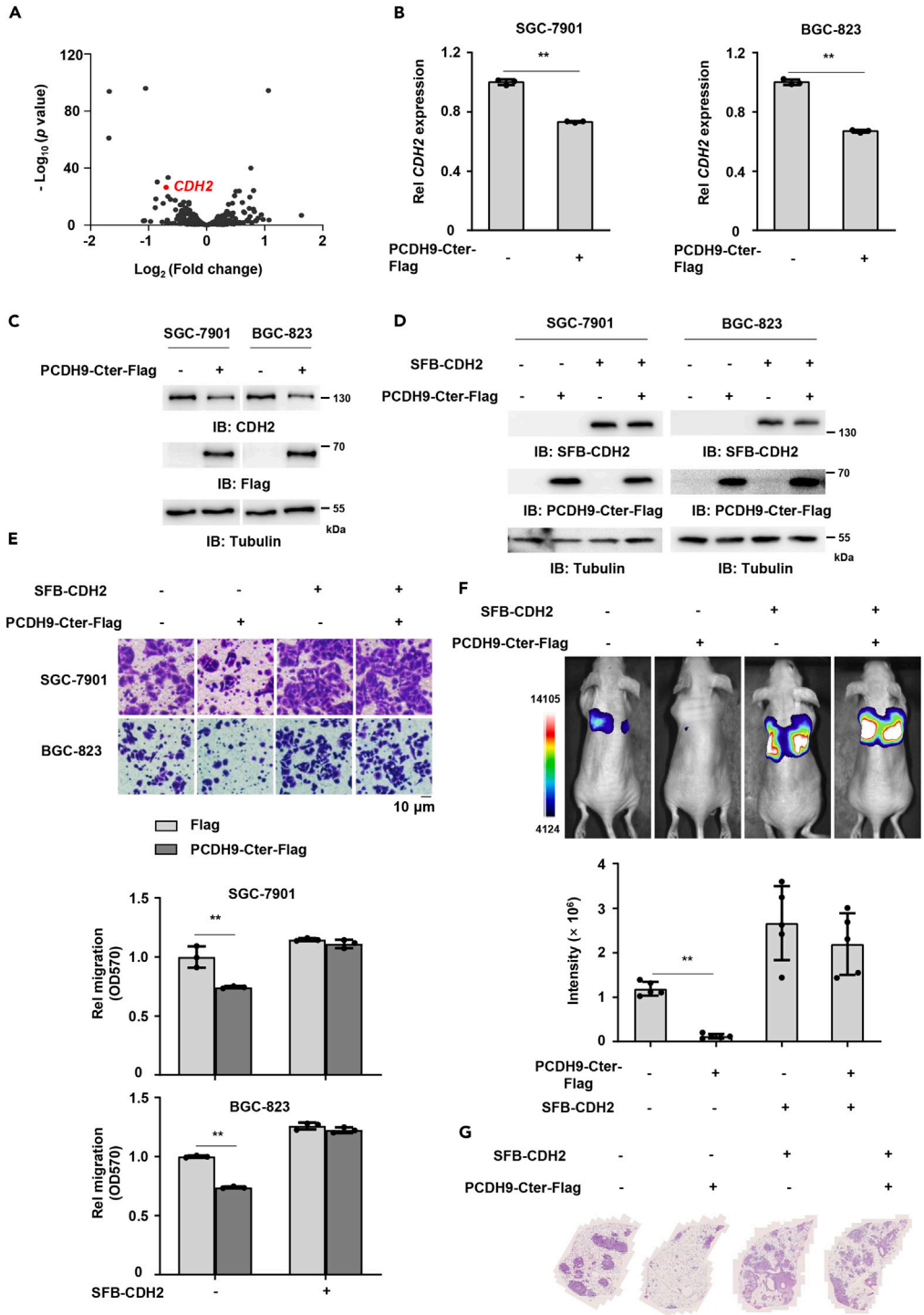

Figure 3. Cleaved PCDH9 C-terminal inhibits the migration and *in vivo* metastasis of gastric cancer cells by downregulating *CDH2* expression

(A) RNA sequencing analyses were performed in BGC-823 cells stably expressing EV or PCDH9-Cter-Flag. Differently expressed genes were presented.

(B) SGC-7901 (left panel) or BGC-823 (right panel) cells were infected with the lentivirus expressing EV or PCDH9-Cter-Flag. The mRNA levels of *CDH2* were examined. Data represents the mean ± SD of three biologically independent experiments (two-tailed Student's *t* test).

(C) SGC-7901 or BGC-823 cells were infected with the lentivirus expressing EV or PCDH9-Cter-Flag. Cells were harvested and immunoblotting analyses were performed.

Figure 3. *Continued*

(D and E) SGC-7901 or BGC-823 cells stably expressing luciferase and EV or PCDH9-Cter-Flag were infected with the lentivirus expressing EV or SFB-CDH2. Cells were harvested and immunoblotting analyses were performed (D). Transwell migration assays were performed in these cells (E). The scale bar represents 10 μm. Representative images (top panel) and statistical analyses (bottom panel) of the migrated cells were shown.

(F and G) SGC-7901 cells stably expressing luciferase and EV or PCDH9-Cter-Flag were infected with the lentivirus expressing EV or SFB-CDH2. Cells were injected into randomized athymic nude mice by tail vein injection (five mice per group). 35 days after inoculation, bioluminescence imaging was performed and representative images of tumor growth were shown (F, top). Data represents mean ± SD of luciferase intensities from five mice (F, bottom; two-tailed Student's *t* test). After bioluminescence imaging, mice were euthanized. Representative images of H&E staining of lung sections from these mice were shown (G). (B, E) Data represents the mean ± SD of three biologically independent experiments (two-tailed Student's *t* test). *p < 0.05, **p < 0.01.

localization signals (NLSs) peptide (Asn866-Ser879) in PCDH9-Cter. We then deleted NLS in PCDH9-Cter and found that NLS deletion blocked nuclear translocation of PCDH9-Cter (Figure S2A). Transwell migration assay showed that in contrast to PCDH9-Cter overexpression, overexpression of PCDH9-Cter with NLS deletion did not influence tumor cell migration (Figure S2B). Collectively, these results demonstrate that nuclear translocation of cleaved PCDH9 inhibits the migration and invasion of gastric cancer cells.

Cleaved PCDH9 C-terminal inhibits the migration and *in vivo* metastasis of gastric cancer cells by downregulating *CDH2* expression

To decipher the mechanism underlying PCDH9-Cter-inhibited tumor cell migration, we performed RNA sequencing analysis for BGC-823 cells with or without PCDH9-Cter overexpression and identified cadherin 2 (*CDH2*), a well-established cell migration promoter,[24] in top 10 migration-related genes that were significantly downregulated (Figure 3A). We first validated *CDH2* expression in SGC-7901 or BGC-823 cells stably expressing empty vector (EV) or PCDH9-Cter-Flag, which showed that PCDH9-Cter-Flag overexpression inhibited mRNA and protein levels of *CDH2* (Figures 3B and 3C).

To test whether CDH2 was required for PCDH9-Cter-inhibited tumor cell migration, we overexpressed CDH2 in luciferase-expressing SGC-7901 or BGC-823 cells stably expressing EV or PCDH9-Cter-Flag (Figure 3D). Transwell migration assay showed that CDH2 overexpression blocked PCDH9-Cter-Flag overexpression-inhibited migration of SGC-7901 or BGC-823 cells (Figure 3E). Moreover, we inoculated these cells into BALB/c nude mice by tail vein injection. Bioluminescence imaging of the mice indicated that PCDH9-Cter overexpression greatly inhibited tumor metastasis, while CDH2 overexpression blocked PCDH9-Cter-Flag overexpression-inhibited tumor metastasis (Figure 3F). The lung nodules were dissected and validated to be metastatic tumors by hematoxylin and eosin (H&E) staining (Figure 3G). Taken together, these results demonstrate that PCDH9-Cter hindered gastric cancer metastasis by downregulating CDH2 expression.

Cleaved PCDH9 C-terminal increases DNA methylation of *CDH2* promoter and therefore inhibits its expression by enhancing DNMT1 activity

To investigate how PCDH9-Cter regulates *CDH2* expression, we performed mass spectrometry analysis of PCDH9-Cter-associated proteins and noticed DNA methyltransferase 1 (DNMT1) in top 15 protein that strongly interacted with PCDH9-Cter (Figure 4A). DNMT1 methylates CpG residues on DNA strands to repress gene expression.[25] We validated their interaction by coimmunoprecipitation (coIP) assays, showing that DNMT1 indeed interacted with PCDH9-Cter (Figure 4B). Besides, the treatment of DNMT1 inhibitor (Azacitidine) blocked PCDH9-Cter-Flag overexpression-repressed CDH2 expression, suggesting that PCDH9-Cter inhibits *CDH2* expression through DNMT1 (Figures 4C and 4D).

To test whether DNMT1 inhibits *CDH2* expression by methylating CpG residues at *CDH2* promoter, we examined DNA methylation status of the CpG islands located upstream (+1,000 bp) of the genomic sequences within the *CDH2* gene. Bisulfate sequencing analysis showed that PCDH9-Cter-Flag overexpression increased DNA methylation status of the CpG islands of *CDH2*, while DNMT1 inhibition blocked PCDH9-Cter-Flag overexpression-induced DNA methylation status of the CpG islands of *CDH2* (Figure 4E). To examine whether PCDH9-Cter regulates DNMT1 activity, we examine DNMT1 activity in SGC-7901 cells expressing EV or PCDH9-Cter-HA, which showed that PCDH9-Cter-HA overexpression increased DNMT1 activity (Figure 4F).

To further confirm the role of DNMT1 in PCDH9-Cter-inhibited gastric cancer migration, we treated BGC-823 cells expressing EV or PCDH9-Cter-Flag with or without DNMT1 inhibitor. Transwell migration assay showed that DNMT1 inhibition blocked PCDH9-Cter-Flag overexpression-inhibited cell migration.

In summary, PCDH9-Cter facilitates CpG methylation of *CDH2* promoter by enhancing DNMT1 activity, thereby inhibiting CDH2 expression and subsequent migration of gastric cancer cells.

Nuclear positive rates of PCDH9 inversely correlate with CDH2 expression in gastric cancer patients

To define the clinical relevance of nuclear PCDH9-regulated CDH2 expression, we performed IHC analysis with anti-PCDH9 (C-terminal) antibody and anti-CDH2 antibody in primary tumor tissues from patients with gastric cancer. The data showed that nuclear positive rates of PCDH9 had a strong inverse correlation with CDH2 levels (Figures 5A and 5B). Besides, we examined the expression of CDH2 in primary tumors and paired metastatic lymph node tumors from 30 gastric cancer patients and found that contrary to nuclear PCDH9, CDH2 expression was higher in metastatic tumors than in primary tumors (Figure 5C). In addition, in metastatic lymph node tumors, nuclear positive rates of PCDH9 had a strong inverse correlation with CDH2 levels (Figure 5D).

A

Accession	Gene names	# PSMs
Q9HC56	PCDH9	12
A0A087WWJ1	MSH6	11
P40222	TXLNA	11
Q1L838	GTBP	11
A0A087X0M4	SLC4A1AP	6
C9JHW1	GIGYF2	6
M0QY97	ZC3H4	6
P46087	NOP2	6
Q6PJY1	FUBP1	6
A0A024R1T4	TNRC6B	5
A0A024R241	NFIL3	5
A0A024R7E3	DNMT1	5
A0A0S2Z5X3	ZGPAT	5
A5PLN4	SF4	5
K7EPP6	ERC1	5

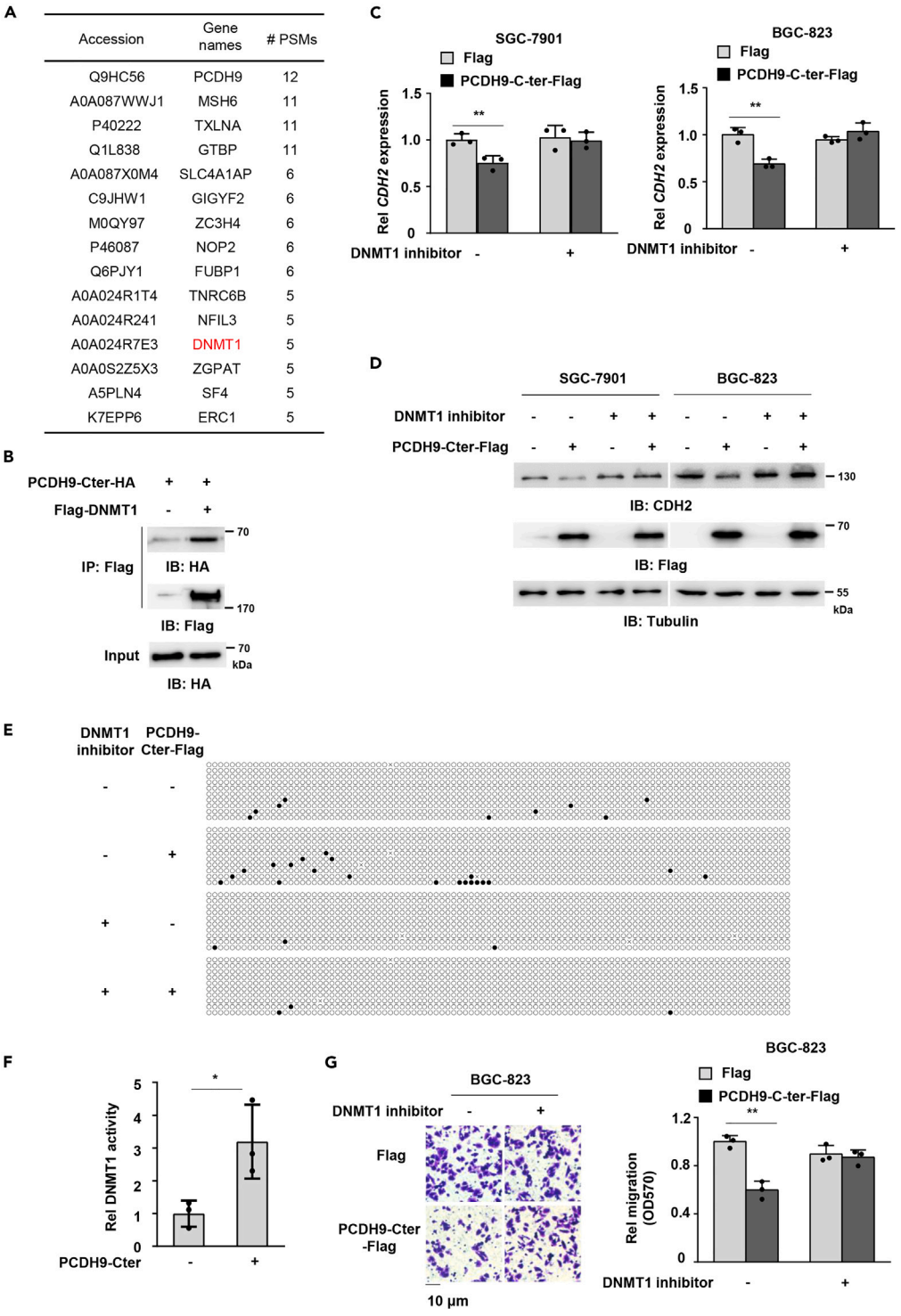

Figure 4. Cleaved PCDH9 C-terminal increases DNA methylation of *CDH2* promoter and therefore inhibits its expression by enhancing DNMT1 activity

(A) Mass spectrometry analyses of PCDH-Cter-associated proteins were performed in BGC-823 cells. The top 15 proteins that showed strong interactions with PCDH-Cter were listed.

(B) BGC-823 cells were co-transfected with EV or Flag-DNMT1 and PCDH9-Cter-HA. IP: immunoprecipitation.

(C and D) SGC-7901 or BGC-823 cells stably expressing EV or PCDH9-Cter-Flag were treated with or without 5 μM DNMT1 inhibitor for 24 h. The mRNA levels (C) and protein levels (D) of *CDH2* were examined.

Figure 4. *Continued*

(E) SGC-7901 cells stably expressing EV or PCDH9-Cter-Flag were treated with or without 5 μM DNMT1 inhibitor for 24 h. DNA methylation in *CDH2* promoter was examined. Open and filled circles represent unmethylated and methylated CpG sites, respectively.

(F) SGC-7901 cells were co-transfected with EV or PCDH9-Cter-HA and Flag-DNMT1. Flag-DNMT1 was immunoprecipitated for DNMT1 activity measurement.

(G) BGC-823 cells stably expressing EV or PCDH9-Cter-Flag were treated with or without 5 μM DNMT1 inhibitor for 24 h. Transwell migration assays were performed in these cells. The scale bar represents 10 μm. Representative images (left panel) and statistical analyses (right panel) of the migrated cells were shown. (C, F, G) Data represent the mean ± SD of three biologically independent experiments (two-tailed Student's *t* test). *$p < 0.05$, **$p < 0.01$.

DISCUSSION

Gastric cancer is one of the leading causes of cancer-related death in both men and women due to delayed diagnosis and high metastatic frequency.[26] Most gastric cancer patients are diagnosed at advanced stages, and consequently some develop metastasis. Metastasis greatly affects the quality of life of gastric cancer patients and is the main cause of cancer-related mortality. Numerous steps are required to establish a metastatic focus, and understanding the molecular mechanisms underlying each step is necessary to conquer metastasis.[27] Cadherins are transmembrane glycoproteins that are responsible for cell-cell adhesion and maintenance of normal tissue architecture. Abnormal cadherins expression is well established to be correlated with adhesion, invasion, and metastasis.[28] PCDHs are a group of transmembrane proteins belonging to the cadherin superfamily. Previous researches showed that PCDHs participated in the development of brain and were involved in some neuronal diseases. Recently, aberrant expression of PCDHs in various human malignant tumors has begun to be revealed. The downregulation or absence of PCDHs was associated with cancer progression.[29] We previously reported that PCDH9 was downregulated during gastric cancer progression. Decreased expression of PCDH9 is frequent in metastatic gastric cancer, and PCDH9 expression is an independent prognostic factor.[16] However, the exact role and molecular mechanism of PCDH9 during gastric cancer metastasis remain unknown. Here we show that PCDH9 is cleaved in gastric cancer. Intracellular domain of PCDH9 translocates into nucleus and interacts with DNMT1 to increase its activity. Highly active DNMT1 increases DNA methylation at *CDH2* promoter to repress its expression, thereby inhibiting tumor cell migration and gastric cancer metastasis (Figure 5E). Our findings reveal a tumor suppressive role of nuclear PCDH9 in gastric cancer metastasis and uncover the mechanism of nuclear PCDH9-inhibited tumor cell migration through DNMT1/CDH2 axis, suggesting a new strategy to inhibit gastric cancer metastasis by promoting nuclear translocation of PCDH9.

In contrast to the function of classical cadherins in cell-cell adhesion, the functions of PCDHs remain elusive.[14] PCDHs have been shown to play important roles in tumorigenesis, tumor cell growth, and tumor cell migration. Hyperactivity of PCDH7 promoted lung tumorigenesis and induced mitogen-activated protein kinase (MAPK) pathway activation in KrasLSL-G12D mutant mice.[30] PCDH-PC promotes androgen-independent prostate cancer cell growth.[31] PCDH8 promotes invasion and metastasis via laminin subunit γ2 in gastric cancer.[32] PCDH9 reduced tumor cell viability, induced apoptosis, and caused G0/G1 cell-cycle arrest in glioma cells.[17] PCDH9 inhibits epithelial-mesenchymal transition and cell migration through activating GSK-3β in hepatocellular carcinoma.[33] In this study, we reveal a new role of nuclear PCDH9 in inhibiting gastric cancer metastasis. In gastric cancer cells, PCDH9 is cleaved and intracellular domain of PCDH9 translocates into nucleus, where it interacts with DNMT1 to increase DNMT1 activity to repress *CDH2* expression, thereby inhibiting tumor cell migration and gastric cancer metastasis. These results uncover the role of PCDH9, especially the intracellular domain of PCDH9, in inhibiting gastric cancer cell migration but also highlight the mechanism of nuclear PCDH9-prevented gastric cancer metastasis by regulating *CDH2* expression.

Furthermore, we investigated the mechanism of nuclear PCDH9-regulated CDH2 expression. We analyzed mass spectrometry data of nuclear PCDH9-associated proteins and found DNMT1 strongly interacting with nuclear PCDH9 (Figure 4A). The DNA methyltransferases (DNMTs) are a conserved family of cytosine methylases with a key role in epigenetic regulation. DNMTs methylate CpG residues to repress gene expression.[25] In this study, we found that nuclear PCDH9 interacts with DNMT1 to increase DNMT1 activity, facilitating *CDH2* promoter CpG methylation to repress *CDH2* expression, ultimately inhibiting gastric cancer metastasis. Our findings demonstrate for the first time that nuclear PCDH9 regulates DNMT1 activity, and the underlying mechanism needs further investigation.

In addition, by analyzing tumor tissues from gastric cancer patients using IHC, we observed that levels of nuclear PCDH9 correlate with levels of CDH2, implicating the importance of nuclear PCDH9-regulated CDH2 in clinical behavior of gastric cancer.

Limitations of the study

The study has identified that PCDH9 undergoes cleavage in gastric cancer cells. The intracellular domain of PCDH9 translocates into the nucleus and enhances DNMT1 activity, leading to the inhibition of *CDH2* expression and tumor metastasis. However, the precise mechanisms underlying PCDH9 cleavage and nuclear translocation are still being investigated. It is worth exploring whether PCDH9 is cleaved by the γ-secretase complex, as PCDH proteins have been frequently shown to be proteolytically cleaved by this complex. Furthermore, the receptor protein responsible for the nuclear translocation of PCDH9 remains unknown. Identifying the specific receptor protein involved in the nuclear translocation of PCDH9 is an important area for future research. Promoting the cleavage and nuclear transportation of PCDH9 by targeting the protease or receptor protein holds the potential to inhibit gastric cancer metastasis. Further investigations are essential to unravel these complexities and advance our understanding of PCDH9-associated mechanisms in cancer metastasis.

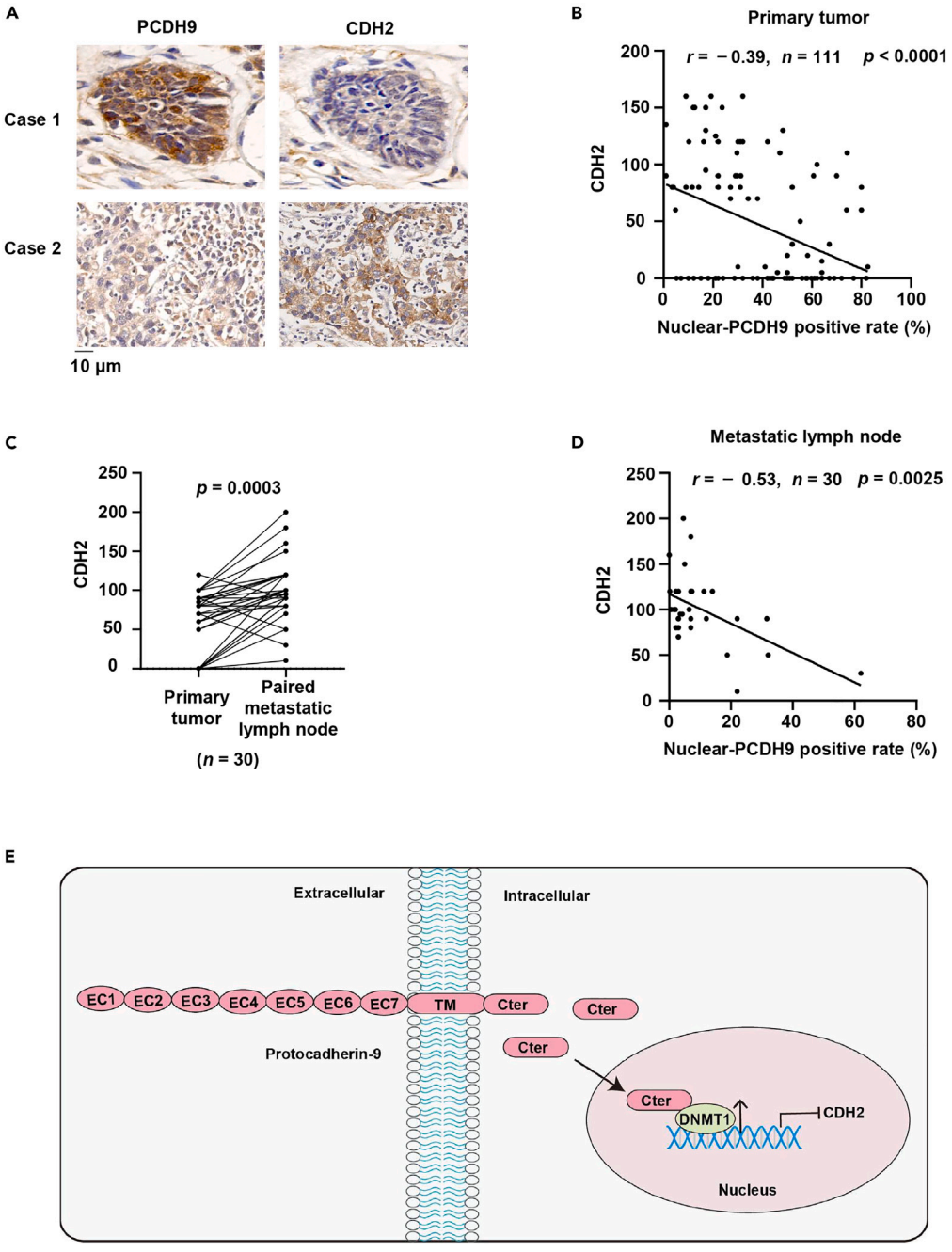

Figure 5. Nuclear positive rates of PCDH9 inversely correlates with CDH2 expression in gastric cancer patients

(A and B) IHC analysis with anti-PCDH9 C-terminal and anti-CDH2 antibodies of 111 specimens from patients with gastric cancer were performed. Representative images of IHC staining of tumors from two gastric cancer patients were shown (A). The scale bar represents 10 μm. Semiquantitative scoring (using a scale from 0 to 300) of CDH2 expression and quantitative scoring of nuclear PCDH9 positive rate were carried out (B, Pearson product moment correlation test; $r = -0.39$, $p < 0.0001$).

(C) IHC staining using anti-CDH2 antibody was performed in primary tumors and paired metastatic lymph node tumors from 30 gastric cancer patients. CDH2 expression were compared between primary tumors and paired metastatic tumors. Semiquantitative scoring was carried out. Data represents the mean ± SD of the two groups (paired, two-tailed Student's *t* test).

Figure 5. *Continued*

(D) IHC analysis with anti-PCDH9 C-terminal and anti-CDH2 antibodies of 30 specimens from metastatic lymph node tumors from 30 gastric cancer patients were performed. Semiquantitative scoring (using a scale from 0 to 300) of CDH2 expression and quantitative scoring of nuclear PCDH9 positive rate were carried out (Pearson product moment correlation test; $r = -0.53$, $p = 0.0025$).

(E) Schematic model of mechanism that nuclear-translocated PCDH9 inhibits gastric cancer metastasis. PCDH9 is cleaved and intracellular domain of PCDH9 (PCDH9-Cter) translocates into nucleus. Nuclear PCDH9 interacts with DNMT1 and increases DNMT1 activity to promote DNA methylation in *CDH2* promoter, inhibiting CDH2 expression and gastric cancer metastasis.

STAR★METHODS

Detailed methods are provided in the online version of this paper and include the following:

- KEY RESOURCES TABLE
- RESOURCE AVAILABILITY
  - Lead contact
  - Materials availability
  - Data and code availability
- EXPERIMENTAL MODEL AND STUDY PARTICIPANT DETAILS
  - Patient specimens
  - Animals
  - Cell culture
- METHOD DETAILS
  - Cell proliferation assay
  - Invasion and migration assays
  - Immunoprecipitation and immunoblotting analysis
  - Subcellular fractionation analysis
  - Mass spectrometry analysis
  - Mouse model of gastric cancer metastasis
  - RNA sequencing analyses
  - Immunohistochemistry
- QUANTIFICATION AND STATISTICAL ANALYSIS
  - Statistical analysis

SUPPLEMENTAL INFORMATION

Supplemental information can be found online at https://doi.org/10.1016/j.isci.2024.109011.

ACKNOWLEDGMENTS

This research was supported by the projects from the National Natural Science Foundation of China (81572856, 81972721) to G.Y.; the Innovative Research Team of High-level Local Universities in Shanghai (SHSMU-ZLCX20212302) to W.Y.; Shanghai Municipal Science and Technology Major Project to W.Y.; Shanghai Science and Technology Development Funds (22QA1409900, 23ZR1470100) to Y. Zhang; the Youth Innovation Promotion Association of the Chinese Academy of Sciences (2022265) to Y. Zhang; National Natural Science Foundation of China (82173306) to Y.C.; and Military Medical Science and Technology Youth Training Program (19QNP036) to J.P.

AUTHOR CONTRIBUTIONS

G.Y., W.Y., and Y. Zhang conceived and designed the study. Y Zhang, Y Zhu, Y.C., and Y.W. performed the experiments. B.L., Y.P., X.L., and J.P. assisted in the animal models. H.G. assisted in reviewing the manuscript. G.Y., W.Y., and Y. Zhang wrote the manuscript with comments from all authors.

DECLARATION OF INTERESTS

The authors declare no competing interests.

Received: September 11, 2023
Revised: December 20, 2023
Accepted: January 22, 2024
Published: February 1, 2024

REFERENCES

1. Huang, R.J., Laszkowska, M., In, H., Hwang, J.H., and Epplein, M. (2023). Controlling Gastric Cancer in a World of Heterogeneous Risk. Gastroenterology *164*, 736–751. https://doi.org/10.1053/j.gastro.2023.01.018.
2. Bray, F., Ferlay, J., Soerjomataram, I., Siegel, R.L., Torre, L.A., and Jemal, A. (2018). Global cancer statistics 2018: GLOBOCAN estimates of incidence and mortality worldwide for 36 cancers in 185 countries. CA. Cancer J. Clin. *68*, 394–424. https://doi.org/10.3322/caac.21492.
3. Chan, W.L., Lam, K.O., Lee, V.H.F., Davidson, M., So, T.H., Li, J.S., Chau, I., and Kwong, D.L.W. (2019). Gastric Cancer - From Aetiology to Management: Differences Between the East and the West. Clin. Oncol. *31*, 570–577. https://doi.org/10.1016/j.clon.2019.05.012.
4. Catalano, V., Labianca, R., Beretta, G.D., Gatta, G., de Braud, F., and Van Cutsem, E. (2005). Gastric cancer. Crit. Rev. Oncol. Hematol. *54*, 209–241. https://doi.org/10.1016/j.critrevonc.2005.01.002.
5. Smyth, E.C., Nilsson, M., Grabsch, H.I., van Grieken, N.C., and Lordick, F. (2020). Gastric cancer. Lancet *396*, 635–648. https://doi.org/10.1016/S0140-6736(20)31288-5.
6. Buzzoni, R., Bajetta, E., Di Bartolomeo, M., Miceli, R., Beretta, E., Ferrario, E., and Mariani, L. (2006). Pathological features as predictors of recurrence after radical resection of gastric cancer. Br. J. Surg. *93*, 205–209. https://doi.org/10.1002/bjs.5225.
7. Valastyan, S., and Weinberg, R.A. (2011). Tumor metastasis: molecular insights and evolving paradigms. Cell *147*, 275–292. https://doi.org/10.1016/j.cell.2011.09.024.
8. Friedl, P. (2019). Rethinking research into metastasis. Elife *8*, e53511. https://doi.org/10.7554/eLife.53511.
9. Fares, J., Fares, M.Y., Khachfe, H.H., Salhab, H.A., and Fares, Y. (2020). Molecular principles of metastasis: a hallmark of cancer revisited. Signal Transduct. Target. Ther. *5*, 28. https://doi.org/10.1038/s41392-020-0134-x.
10. Nieto, M.A., Huang, R.Y.J., Jackson, R.A., and Thiery, J.P. (2016). Emt: 2016. Cell *166*, 21–45. https://doi.org/10.1016/j.cell.2016.06.028.
11. Chiang, A.C., and Massagué, J. (2008). Molecular basis of metastasis. N. Engl. J. Med. *359*, 2814–2823. https://doi.org/10.1056/NEJMra0805239.
12. Mountzios, G., Pentheroudakis, G., and Carmeliet, P. (2014). Bevacizumab and micrometastases: revisiting the preclinical and clinical rollercoaster. Pharmacol. Ther. *141*, 117–124. https://doi.org/10.1016/j.pharmthera.2013.09.003.
13. Steeg, P.S. (2016). Targeting metastasis. Nat. Rev. Cancer *16*, 201–218. https://doi.org/10.1038/nrc.2016.25.
14. Kim, S.Y., Yasuda, S., Tanaka, H., Yamagata, K., and Kim, H. (2011). Non-clustered protocadherin. Cell Adh. Migr. *5*, 97–105. https://doi.org/10.4161/cam.5.2.14374.
15. Ren, S., Wei, G.H., Liu, D., Wang, L., Hou, Y., Zhu, S., Peng, L., Zhang, Q., Cheng, Y., Su, H., et al. (2018). Whole-genome and Transcriptome Sequencing of Prostate Cancer Identify New Genetic Alterations Driving Disease Progression. Eur. Urol. *73*, 322–339. https://doi.org/10.1016/j.eururo.2017.08.027.
16. Chen, Y., Xiang, H., Zhang, Y., Wang, J., and Yu, G. (2015). Loss of PCDH9 is associated with the differentiation of tumor cells and metastasis and predicts poor survival in gastric cancer. Clin. Exp. Metastasis *32*, 417–428. https://doi.org/10.1007/s10585-015-9712-7.
17. Wang, C., Tao, B., Li, S., Li, B., Wang, X., Hu, G., Li, W., Yu, Y., Lu, Y., and Liu, J. (2014). Characterizing the role of PCDH9 in the regulation of glioma cell apoptosis and invasion. J. Mol. Neurosci. *52*, 250–260. https://doi.org/10.1007/s12031-013-0133-2.
18. Lv, J., Zhu, P., Zhang, X., Zhang, L., Chen, X., Lu, F., Yu, Z., and Liu, S. (2017). PCDH9 acts as a tumor suppressor inducing tumor cell arrest at G0/G1 phase and is frequently methylated in hepatocellular carcinoma. Mol. Med. Rep. *16*, 4475–4482. https://doi.org/10.3892/mmr.2017.7193.
19. Zhang, J., Yang, H.Z., Liu, S., Islam, M.O., Zhu, Y., Wang, Z., and Chen, R. (2022). PCDH9 suppresses melanoma proliferation and cell migration. Front. Oncol. *12*, 903554. https://doi.org/10.3389/fonc.2022.903554.
20. Bonn, S., Seeburg, P.H., and Schwarz, M.K. (2007). Combinatorial expression of alpha- and gamma-protocadherins alters their presenilin-dependent processing. Mol. Cell Biol. *27*, 4121–4132. https://doi.org/10.1128/MCB.01708-06.
21. Haas, I.G., Frank, M., Véron, N., and Kemler, R. (2005). Presenilin-dependent processing and nuclear function of gamma-protocadherins. J. Biol. Chem. *280*, 9313–9319. https://doi.org/10.1074/jbc.M412909200.
22. Fortini, M.E. (2002). Gamma-secretase-mediated proteolysis in cell-surface-receptor signalling. Nat. Rev. Mol. Cell Biol. *3*, 673–684. https://doi.org/10.1038/nrm910.
23. Nguyen Ba, A.N., Pogoutse, A., Provart, N., and Moses, A.M. (2009). NLStradamus: a simple Hidden Markov Model for nuclear localization signal prediction. BMC Bioinf. *10*, 202. https://doi.org/10.1186/1471-2105-10-202.
24. Cao, Z.Q., Wang, Z., and Leng, P. (2019). Aberrant N-cadherin expression in cancer. Biomed. Pharmacother. *118*, 109320. https://doi.org/10.1016/j.biopha.2019.109320.
25. Lyko, F. (2018). The DNA methyltransferase family: a versatile toolkit for epigenetic regulation. Nat. Rev. Genet. *19*, 81–92. https://doi.org/10.1038/nrg.2017.80.
26. Huang, T., Song, C., Zheng, L., Xia, L., Li, Y., and Zhou, Y. (2019). The roles of extracellular vesicles in gastric cancer development, microenvironment, anti-cancer drug resistance, and therapy. Mol. Cancer *18*, 62. https://doi.org/10.1186/s12943-019-0967-5.
27. Shimizu, D., Kanda, M., and Kodera, Y. (2018). Emerging evidence of the molecular landscape specific for hematogenous metastasis from gastric cancer. World J. Gastrointest. Oncol. *10*, 124–136. https://doi.org/10.4251/wjgo.v10.i6.124.
28. Kaszak, I., Witkowska-Piłaszewicz, O., Niewiadomska, Z., Dworecka-Kaszak, B., Ngosa Toka, F., and Jurka, P. (2020). Role of Cadherins in Cancer-A Review. Int. J. Mol. Sci. *21*, 7624. https://doi.org/10.3390/ijms21207624.
29. Shan, M., Su, Y., Kang, W., Gao, R., Li, X., and Zhang, G. (2016). Aberrant expression and functions of protocadherins in human malignant tumors. Tumour Biol. *37*, 12969–12981. https://doi.org/10.1007/s13277-016-5169-9.
30. Zhou, X., Padanad, M.S., Evers, B.M., Smith, B., Novaresi, N., Suresh, S., Richardson, J.A., Stein, E., Zhu, J., Hammer, R.E., and O'Donnell, K.A. (2019). Modulation of Mutant Kras(G12D) -Driven Lung Tumorigenesis In Vivo by Gain or Loss of PCDH7 Function. Mol. Cancer Res. *17*, 594–603. https://doi.org/10.1158/1541-7786.MCR-18-0739.
31. Terry, S., Queires, L., Gil-Diez-de-Medina, S., Chen, M.W., de la Taille, A., Allory, Y., Tran, P.L., Abbou, C.C., Buttyan, R., and Vacherot, F. (2006). Protocadherin-PC promotes androgen-independent prostate cancer cell growth. Prostate *66*, 1100–1113. https://doi.org/10.1002/pros.20446.
32. Lin, Y., Ge, X., Zhang, X., Wu, Z., Liu, K., Lin, F., Dai, C., Guo, W., and Li, J. (2018). Protocadherin-8 promotes invasion and metastasis via laminin subunit gamma2 in gastric cancer. Cancer Sci. *109*, 732–740. https://doi.org/10.1111/cas.13502.
33. Zhu, P., Lv, J., Yang, Z., Guo, L., Zhang, L., Li, M., Han, W., Chen, X., Zhuang, H., and Lu, F. (2014). Protocadherin 9 inhibits epithelial-mesenchymal transition and cell migration through activating GSK-3beta in hepatocellular carcinoma. Biochem. Biophys. Res. Commun. *452*, 567–574. https://doi.org/10.1016/j.bbrc.2014.08.101.
34. Zhang, Y., Yu, G., Chu, H., Wang, X., Xiong, L., Cai, G., Liu, R., Gao, H., Tao, B., Li, W., et al. (2018). Macrophage-Associated PGK1 Phosphorylation Promotes Aerobic Glycolysis and Tumorigenesis. Mol. Cell *71*, 201–215.e7. https://doi.org/10.1016/j.molcel.2018.06.023.
35. Wang, X., Liu, R., Zhu, W., Chu, H., Yu, H., Wei, P., Wu, X., Zhu, H., Gao, H., Liang, J., et al. (2019). UDP-glucose accelerates SNAI1 mRNA decay and impairs lung cancer metastasis. Nature *571*, 127–131. https://doi.org/10.1038/s41586-019-1340-y.
36. Wu, Y.B., Dai, J., Yang, X.L., Li, S.J., Zhao, S.L., Sheng, Q.H., Tang, J.S., Zheng, G.Y., Li, Y.X., Wu, J.R., and Zeng, R. (2009). Concurrent quantification of proteome and phosphoproteome to reveal system-wide association of protein phosphorylation and gene expression. Mol. Cell. Proteomics *8*, 2809–2826. https://doi.org/10.1074/mcp.M900293-MCP200.

STAR★METHODS

KEY RESOURCES TABLE

REAGENT or RESOURCE	SOURCE	IDENTIFIER
Antibodies		
Rabbit monoclonal anti-PCDH9 N terminal	Santa Cruz Biotechnology	sc-84563; RRID: AB_2158843
Rabbit monoclonal anti-PCDH9 C terminal	Santa Cruz Biotechnology	sc-84564; RRID: RRID: AB_2251922
Mouse monoclonal anti-Flag	Sigma-Aldrich	F1804; RRID: AB_262044
Mouse monoclonal anti-Tubulin	Sigma-Aldrich	T5201; RRID: AB_609915
Rabbit monoclonal anti-Lamin B1	Cell Signaling Technology	13435; RRID: AB_2737428
Rabbit polyclonal anti-CDH2	Proteintech Group	22018-1-AP; RRID: AB_2813891
Rabbit monoclonal anti-HA	Cell Signaling Technology	3724; RRID: AB_1549585
anti-Flag M2 affinity gel	Sigma-Aldrich	A2220; RRID:AB_10063035
Bacterial and virus strains		
Trans1-T1	Transgene Biotech	CD501-03
Biological samples		
Human gastric cancer specimens	Shanghai Changhai Hospital	N/A
Chemicals, peptides, and recombinant proteins		
Puromycin	EMD Biosciences	540222
D-luciferin	PerkinElmer	122799
Azacitidine	Selleck	S1782
Flag peptide	Abclonal Technology	peptide0001
Critical commercial assays		
ReverTra Ace qPCR RT Master Mix Kit	Toyobo	FSQ-301
Cell Counting Kit-8	Selleck	B34302
Methyltransferase assay kit	Promega	V7601
Deposited data		
Raw data of immunoblotting images	Mendeley data	https://doi.org/10.17632/fh85jkc9yt.1
RNA sequencing data	GEO	GSE248874
Experimental models: Cell lines		
Human: SGC-7901	Longhua Hospital Affiliated to Shanghai University of Traditional Chinese Medicine	N/A
Human BGC-823	Longhua Hospital Affiliated to Shanghai University of Traditional Chinese Medicine	N/A
Experimental models: Organisms/strains		
Mouse: BALB/c nude	Lingchang Biotech	N/A
Oligonucleotides		
PCDH9 siRNA: CCUGUUGGCUGCUCUGAUU	GenePharma	N/A
Non-targeting siRNA: UUCUCCGAACGUGUCACGU	GenePharma	N/A
Recombinant DNA		
pcDH/puro(+)-PCDH9-Flag	This paper	N/A
pcDH/puro(+)-PCDH9-(EC7-Cter)-Flag	This paper	N/A
pcDH/puro(+)-PCDH9-(TM-Cter)-Flag	This paper	N/A
pcDH/puro(+)-PCDH9 Cter-Flag	This paper	N/A

(*Continued on next page*)

Continued

REAGENT or RESOURCE	SOURCE	IDENTIFIER
pcDNA3.1/hygro(+)-PCDH9 Cter-HA	This paper	N/A
pcDH/puro(+)-PCDH9-Cter-delNLS-Flag	This paper	N/A
pcDNA4-Flag-DNMT1	Guoliang Xu lab; Center for Excellence in Molecular Cell Science, Chinese Academy of Sciences	N/A
Software and algorithms		
Graphpad Prism	GraphPad	https://www.graphpad.com/support

RESOURCE AVAILABILITY

Lead contact

Further information and requests for resources and reagents should be directed to and will be fulfilled by the Lead Contact, Guanzhen Yu (qiaoshanqian@aliyun.com).

Materials availability

The materials underlying this article will be shared upon request to the lead contact.

Data and code availability

The RNA sequencing data reported in this paper have been deposited in the Gene Expression Omnibus (GEO) database. The accession number for the RNA sequencing data reported in this paper is GSE248874. Raw data of immunoblotting images have been deposited to Mendeley Data and are available at https://doi.org/10.17632/fh85jkc9yt.1. Thess data are publicly available as of the date of publication. This study does not report original code.

Any additional information required to reanalyze the data reported in this paper is available from the lead contact upon request.

EXPERIMENTAL MODEL AND STUDY PARTICIPANT DETAILS

Patient specimens

135 patients with primary gastric cancer without preoperative chemotherapy or radiotherapy from East Asian were enrolled in this study. Among these patients, 91 patients (67.4%) are male and 44 patients (32.6%) are female. The median age was 57 years old (ranging from 20 to 80). Of the 135 cases, 25 patients (18.5%) had TNM stage I tumors, 21 patients (15.6%) had TNM stage II tumors, 63 patients (46.7%) had TNM stage III tumors, 26 patients (19.3%) had TNM stage IV tumors. 38 patients (28.1%) were diagnosed without lymph node metastasis, while 97 patients (71.9%) were with lymph node metastasis. 111 of the 135 patients were available for follow-up, with a median follow-up of 59 months (3-69 months). Among the 135 patients, 30 cases had matched metastatic lymph nodes. The institutional review boards of Shanghai Changhai Hospital, Naval Medical University approved the use of these tissues and clinical information. Informed consent was obtained from all patients.

Animals

6-week-old female BALB/c athymic nude mice were used. All mice were maintained in pathogen-free facilities at the Shanghai Institute of Biochemistry and Cell Biology (SIBCB). Animals were randomly allocated to experimental groups. The animal experiments were performed in a blinded manner. All animal experiments were approved by the Institutional Animal Care and Use Committee (IACUC) of Shanghai Institute of Biochemistry and Cell Biology, Chinese Academy of Sciences and complied with all relevant ethical regulations. Tumor sizes in all experiments are within the limit permitted by the SIBCB IACUC.

Cell culture

The human gastric cancer cell lines SGC-7901 and BGC-823 were obtained from Longhua Hospital Affiliated to Shanghai University of Traditional Chinese Medicine. Cells were maintained in Dulbecco's modified Eagle's medium (DMEM) supplemented with 10% fetal bovine serum (FBS) and antibiotics. Cells were incubated in 5% CO_2 at 37°C. All cell lines were authenticated using the short tandem repeat (STR) method and were tested negative for mycoplasma.

METHOD DETAILS

Cell proliferation assay

1000 cells per well were plated in 96-well plate and cultured for indicated days. Cell proliferation was evaluated using the Cell-Counting Kit 8 (CCK8, Selleck).

Invasion and migration assays

Invasion assays were performed in 8 μm-pore transwell inserts with coated Matrigel, as instructed by the manufacturer (BD Biosciences, San Jose, CA). A total of 1×10^5 cells were seeded in the upper chamber with serum-free medium while the bottom chambers were filled with medium containing 10% FBS. After 24 hours, the invaded cancer cells were stained with crystal violet, followed by solubilization of crystal violet with 100 μL 33% acetic acid. Invasion ability was determined by optical density (OD570) measurement. Migration assay was performed the same as invasion assay without coated Matrigel. Data represents the mean ± SD of three independent experiments.

Immunoprecipitation and immunoblotting analysis

Extraction of proteins with a modified buffer from cultured cells was followed by immunoprecipitation and immunoblotting with corresponding antibodies.[34]

Subcellular fractionation analysis

SGC-7901 or BGC-823 cells were collected and washed three times with cold PBS. Nuclear or cytosolic fractions were prepared using the Nuclear Extract Kit (Active Motif).

Mass spectrometry analysis

PCDH9-Cter-Flag proteins were immunoprecipitated from BGC-823 cells. The precipitated complexes were boiled at 95 °C for 10 min. PCDH9-Cter and PCDH9-Cter-associated proteins were separated using SDS-PAGE. The fractions were processed as described,[35] such as reductive alkylation, trypsin digestion and peptide extraction. The peptides were analyzed by liquid chromatography–tandem mass spectrometry on a Q Exactive mass spectrometer (Thermo Fisher Scientific).

Proteins were identified by a database search of the fragment spectra against the National SwissProt protein database (EBI) using Mascot Server 2.4 (Matrix Science).[36]

Mouse model of gastric cancer metastasis

In brief, 2×10^6 (in 100 μL of PBS per mouse) luciferase-expressing SGC-7901 cells were injected into randomized 6-week-old female athymic nude mice through the lateral tail vein. Five mice per group were used. After inoculation for 35 days, bioluminescence imaging of tumor metastasis was carried out using Tanon-5200 Chemiluminescent Imaging System (Tanon, China). Then animals were euthanized and the lungs were dissected and fixed in 4% formaldehyde. Haematoxylin and eosin (H&E) staining were performed on the lung sections. The metastatic nodules were found according to the H&E staining of the lung sections.

RNA sequencing analyses

Briefly, BGC-823 cells (1×10^6) stably expressing Flag vector or PCDH9-Cter-Flag were collected and RNA of the collected cells was extracted with Trizol reagent (Life technologies). Then the RNA sequencing analyses was performed by Berry Genomics (Beijing, China).

Immunohistochemistry

The tissue sections from paraffin-embedded human gastric tumors were stained with antibodies as indicated. We quantitatively scored the tissue sections according to the percentage of positive cells and staining intensity. The score (H-score) was obtained using the formula: H-score = Σ (Pi × i), where "Pi" represents the percentage of cells falling within specific staining intensity categories, and "i" denotes the intensity score assigned to each category. Typically, these intensity scores correspond to numerical values, with 0 indicating no staining, 1 for weak staining, 2 for moderate staining, and 3 for strong staining.

QUANTIFICATION AND STATISTICAL ANALYSIS

Statistical analysis

No statistical methods were used to predetermine sample size. A log-rank test was used to analyze the statistical significance of the survival correlations between groups (Figure 1A). A paired, two-tailed Student's *t*-test was used for two-group comparisons (Figures 1B and 5C). A Pearson's correlation test was used to analyze the statistical significance of the correlation of CDH2 expression and nuclear-PCDH9 positive rate in the human gastric cancer (Figures 5B and 5D). An unpaired, two-tailed Student's *t*-test was used for two-group comparisons other than the analyses mentioned above. Data represents the mean ± SD of three biologically independent experiments (two-tailed Student's *t*-test). $*p < 0.05$, $**p < 0.01$.